

# Microscopic simulation of short pulse laser damage of melanin particles

Leonid V. Zhigilei and Barbara J. Garrison

*Department of Chemistry, 152 Davey Laboratory, Penn State University, University Park, PA 16802*

## Abstract

Microscopic mechanisms of short pulse laser damage to melanin granules, the strongest absorbing chromophores of visible and near - IR light in the retina and skin, are studied using the molecular dynamics simulations. The pulse width dependence of the fracture/cavitation and vaporization processes within the small particles, their coupling to the surrounding medium and the resulting tissue injury are discussed based on the simulation results. The effect of laser irradiation on an isolated submicron particle at different laser fluences and pulse durations is first analyzed. The mechanical disruption of the particle due to the laser induced pressure is found to define the character of damage for short pulse widths (tens of picoseconds) at laser fluences that are significantly lower than those required for boiling. Thermal relaxation and explosive disintegration of the overheated particle at higher laser fluencies are the processes that dominate at longer laser pulses (hundreds of picoseconds). Damage of an absorbing particle embedded into a transparent medium with different mechanical characteristics is then simulated. Coupling of the acoustic and thermal pulses generated within absorbing particles to the surrounding medium is studied and the possible cumulative effects from an ensemble of absorbing particles are discussed. The simulation results provide the basis for future work in which the microscopic and continuum descriptions are combined for multiscale modeling of laser tissue interaction.

**Keywords:** computer simulation, melanin, pressure waves, photomechanical damage

## 1. Introduction

Computer simulations have been shown to enhance our understanding of the elementary processes occurring in a wide range of physical phenomena. The simulations are especially beneficial in the cases when important processes occurs at the time or length-scales inaccessible for direct experimental investigation. This is the case for the short pulse laser injury to epithelial (pigmented) tissues of the eye and skin where the laser energy is absorbed within micrometer-sized melanosomes composed of strongly absorbing granules of the biological pigment melanin with dimension of order 10-15 nm. The processes within the absorbing granules and their coupling to the surrounding transparent medium should be understood in order to predict the cumulative effect from all granules in the melanosome and the character of the resulting laser damage of the tissue.

The effects of the thermal and stress confinement within melanin granules or the whole melanosome have been discussed theoretically,<sup>1,2</sup> investigated experimentally,<sup>3,4</sup> and simulated using a continuum hydrodynamic model.<sup>5</sup> For sub-nanosecond pulses, the spatially non-uniform absorption and hot spot formation within the melanosome are the factors that are presumably responsible for the substantially lower threshold for minimal visible tissue damage than with longer laser pulses. It has been proposed that relation between the size of the melanin granules and the laser pulse duration is the critical factor that defines the mechanism of short pulse laser injury.<sup>1</sup> When laser pulse duration  $\tau_p$  becomes shorter than the time for cooling of the absorbing granule by thermal conduction, the hot spots are formed at and around the absorber. Explosive vaporization of the overheated granule and/or the surrounding medium can lead to the vapor bubble formation and generation of a pressure wave.<sup>3,4,5</sup> Moreover, when  $\tau_p$  is shorter than the time of mechanical relaxation of the stresses generated due to the fast heating of the granule, a high pressure can build up within the absorbing structure at low laser fluences when the deposited energy is below the threshold for explosive vaporization.<sup>1</sup> The emission of strong shock waves from melanosomes isolated in water and irradiated with 40 and 100 ps laser pulses have been observed experimentally<sup>3,4</sup> and reproduced in computer simulations.<sup>5</sup> These observations suggest the importance of photomechanical effects in the short pulse laser damage to pigmented tissues. What is lacking, however, is the information on microscopic mechanisms and nature of the laser induced damage at submicron scale. The complexity and diversity of the processes that define the tissue damage, namely, formation and development of laser induced pressure within and outside the absorbing granules, nucleation, growth, and

interaction of microcracks and cavities, explosive vaporization, spinodal decomposition and cooling of the overheated material, hinder the analytical description of the phenomenon.

An alternative method of microscopic analysis of laser induced processes is the molecular dynamics (MD) computer simulation technique.<sup>6</sup> The advantage of this approach is that only details of the microscopic interactions need to be specified, and no assumptions are made about the character of the processes under study. Rather the physical phenomena arise naturally out of the simulations. Moreover, the MD method is capable of providing a complete microscopic description of the dynamic processes induced by the laser pulse as well as the final results of the laser irradiation. Recent development of a breathing sphere model for MD simulations of laser ablation<sup>7</sup> have significantly expanded the time and length scales of the model and have laid the foundation for bridging the gap between the microscopic and mesoscopic aspects of laser ablation and damage of organic solids. Application of the model to the analysis of the ablation of molecular films and matrix-assisted laser desorption demonstrate the ability of the method to provide insight into the microscopic mechanisms of laser ablation.<sup>7,8,9</sup>

In this work, we use the MD method and the breathing sphere model to investigate the basic processes and mechanisms that define a strong dependence on pulse duration of the threshold energy for producing a minimal visible damage to pigmented tissues. Irradiation of individual submicron particles and absorbing particles embedded into a transparent medium is simulated at laser fluences close to the threshold for damage. Apparent qualitative differences in the damage mechanisms for shorter, tens of picoseconds, and longer, hundreds of picoseconds, laser pulses are delineated and related to the experimental observations for pigmented tissues.

## **2. Computational Method**

The molecular dynamics computer simulation technique is used in this work to investigate microscopic mechanisms of short pulse laser damage to absorbing particles embedded in a transparent medium. We study the effects of laser irradiation at submicron resolution that is inaccessible for neither the traditional atomic level MD nor continuum simulations.<sup>5,10</sup> Two innovations are used to expand the time of the MD simulation and the size of the simulated system. These are the breathing sphere model for molecular dynamics simulations of laser ablation and damage in organic materials and non-reflecting boundary conditions that allows us to simulate the propagation of the laser induced stress waves out from the MD computational cell.

**The breathing sphere model.** The model and the results relevant to the application of the laser ablation phenomena in mass spectrometry are described in detail elsewhere.<sup>7,8,9</sup> Briefly, the model assumes that each molecule (or appropriate group of atoms) can be represented by a single particle that has the true translational degrees of freedom but an approximate internal degree of freedom. This internal (breathing) mode allows us to reproduce a realistic rate of the conversion of internal energy of the molecules excited by the laser to the translational motion of the other molecules. Because we are following molecules and not atoms, our system size can be significantly larger. Moreover, because we are not following explicit atomic vibrations our timestep in the numerical integration is longer. Molecular level resolution of the material description provides an easy means for simulation of complex inhomogeneous organic materials. The strength of the material, the bonding interactions, as well as the wavelength dependent absorptivity of the different tissue components can be easily included. The rate of energy transfer within an individual tissue component as well as between components can be precisely controlled.<sup>7</sup>

**Non-reflecting boundary conditions.** The generation of stress waves is a natural result of the fast energy deposition in the case of short pulse laser irradiation and inhomogeneous absorption.<sup>1,3,4,5,7,8,10,11</sup> Simulation of the propagation of the stress waves requires the size of the MD computational cell to be increased linearly with the time of the simulation. For times longer than ~100 ps the size of the model required to follow the wave propagation becomes computationally prohibitive. On the other hand, since displacements of the molecules in a region outside the immediate vicinity of the absorbing granule are small, the propagation of the laser induced stress waves can be readily described at the continuum level and do not require a molecular level analysis. In this work the non-reflecting propagation of the stress wave out from the MD computational cell is simulated using recently developed boundary conditions where the traveling wave equation is used to obtain the forces acting at the molecules in the boundary region.<sup>12</sup> The formation and propagation of the pressure wave within the MD computational cell as well as out from the MD region through the non-reflecting boundary is illustrated in Figure 1 for the simulation set up used in Ref. 7-9. In this case the high pressure builds up during the 15 ps laser pulse within the penetration depth of the irradiated sample. The high pressure causes ablation of a part of the irradiated volume and drives a strong compression wave into the bulk of the sample. The non-reflecting boundary conditions set at the

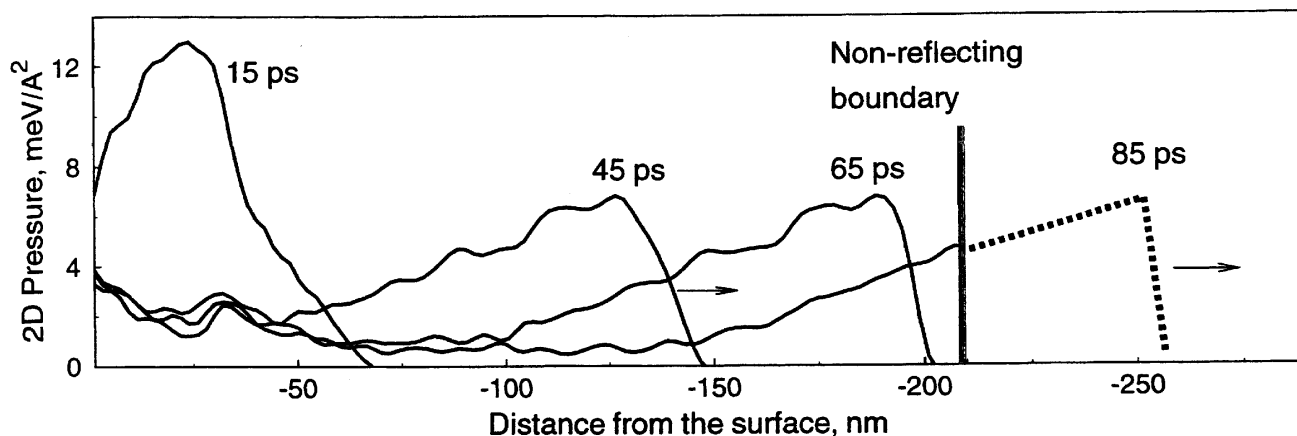


Figure 1. The time development of the high pressure within the penetration depth, 32 nm, of the irradiated sample and propagation of the pressure wave into the bulk of the sample. Non-reflecting boundary conditions set at the depth of 210 nm are used to mimic the propagation of the wave through the boundary of the MD computational cell as schematically shown by dashed line.

depth of 210 nm allow us to avoid an unphysical reflection of the pressure wave from the boundary of the MD computational cell and to monitor the amount of energy carried away by the wave.<sup>12</sup>

**Simulation setup.** An accurate molecular level simulation of the laser induced damage in a cell requires the knowledge of structural, mechanical, optical, and thermodynamic properties of subcellular structures. As of now, these properties cannot be reliably ascertained from the available experimental data. For example, particles described by a water equation of state and solid protein granules were both considered as possible alternative representations of melanin granules in recent simulations of Strauss et al.<sup>5</sup> Due to uncertainty in sizes, structures and mechanical properties of the submicron compounds we choose to use the present simulations to address general mechanisms and dynamics of short pulse laser damage from inhomogeneous absorption in tissue. As a first step we perform simulations for an isolated melanin granule and study the effect of the mechanical characteristics of the surrounding medium on the laser induced processes.

Simulations are performed both on a two-dimensional (2D) and a three-dimensional (3D) versions of the breathing sphere model. The 2D simulation offers a clear visual picture of the damage process whereas 3D model has a potential for a quantitative comparison between the computed and experimental results. The parameters of the model used to represent an organic solid are given elsewhere.<sup>7</sup> Two-dimensional simulations have been performed for an absorbing particle with radius of 55 nm consisting of 33,799 molecules. We perform simulations both for isolated particles and particles embedded into a transparent medium. The computational setup for the latter case is shown in Figure 2. In this setup the MD computational cell has an outer radius of 140 nm and consists of 220,525 molecules. Non-reflecting boundary conditions are applied at the border of the computational cell in order to mimic the propagation of the laser induced pressure waves through the border. To study the role of the acoustic impedance mismatch at the interface between the absorbing granule and the surrounding medium, simulations are performed with two sets of parameters for intermolecular interactions in the surrounding medium. With one set the granule and the surrounding medium have identical

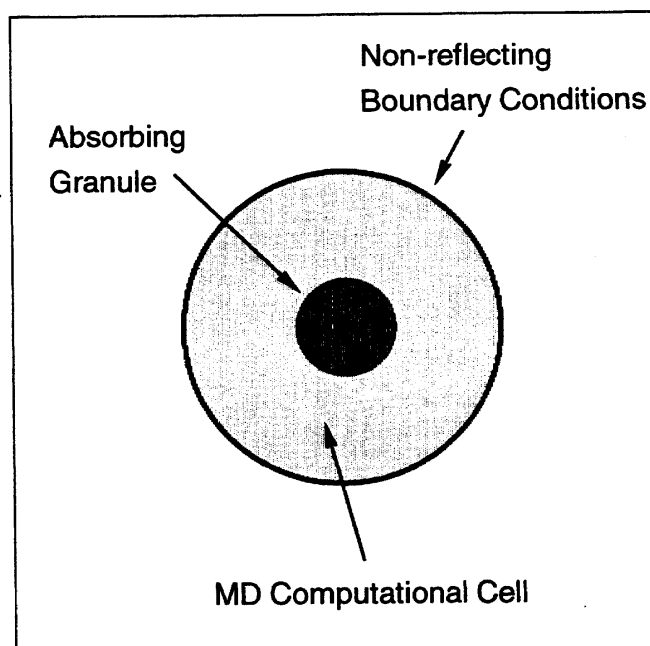


Figure 2. Schematic sketch of the simulation setup.

mechanical properties, with another set intermolecular interactions in the surrounding medium are half as much leading to ~30% mismatch in the acoustic impedance at the interface between the particle and surrounding medium. For the 3D simulations we use an amorphous molecular cluster with the radius of 10 nm consisting of 28,955 molecules. Parameters of the 3D model are chosen to reproduce the density,  $\rho$ , of 1.2 g/cm<sup>3</sup> and sound velocity,  $c_s$ , of 1650 m/s in the granule.

The laser irradiation is simulated by vibrational excitation of molecules that are randomly chosen during the laser pulse duration. In this case an implicit assumption is that the particle absorbs homogeneously and the effect of laser beam attenuation within the particle can be neglected. The vibrational excitations are performed by depositing a quantum of energy equal to the photon energy into the kinetic energy of internal vibration of the molecule to be excited.<sup>7</sup> Laser pulses of 10 ps and 100 ps in duration at a wavelength of 337 nm are used in the 3D simulations. In 2D simulations pulses of 15 ps and 300 ps are used and the photon energy is scaled down by factor of two in order to account for the lower cohesive energies in the 2D system as compared to the 3D case. A series of simulations at different laser fluences is performed for each pulse duration, starting from a fluence that does not cause any visible damage to the absorbing particle up to fluences that lead to significant visible damage to the particle.

**Analysis of simulation results.** The MD simulation technique allows one to perform a detailed analysis of the laser induced processes. In particular, visual observations can be correlated with data on microscopic dynamics at the molecular level. The positions, velocities, and energies of molecules are obtained directly from the MD algorithm. The concept of local atomic stresses<sup>13</sup> is used in calculations of the local hydrodynamic pressure that is defined as a first invariant of the stress tensor. The coordination numbers of molecules defined through the Dirichlet construction are used to characterize the defect structure and describe the structural changes and phase transitions occurring in the 2D model.<sup>7,14</sup>

### 3. Results

In this section we start from the simulation results for isolated absorbing particles. The damage mechanism and the laser fluence threshold values for producing minimal damage within a particle are compared for irradiation with laser pulses of different durations. The physical processes and mechanisms leading to the apparent pulse duration dependence of particle damage are analyzed. Coupling of the acoustic and thermal pulses generated within absorbing particles to the surrounding medium is then studied and the role of the acoustic impedance mismatch between the absorbing granule and the surrounding medium is discussed.

#### 3.1 Isolated particles. Mechanical disruption vs thermal disintegration.

Snapshots from the 2D simulations given in Figure 3 clearly indicate that the laser fluence threshold values for producing minimal damage or cavitation within an isolated particle are essentially different for irradiation with 300 ps and 15 ps pulses. For the 15 ps laser pulse, the threshold laser fluence for producing a minimal visible damage to the irradiated particle is found to correspond to ~0.12 eV per molecule within the particle, Figure 3a. The damage at the threshold has a pronounced character of mechanical disruption of a relatively cold particle. We find that at about 50 ps (or 35 ps after the end of the pulse) a cluster of microcracks is generated. All the microcracks originate in the central part of the particle and radiate outward from the center. Within the succeeding 500 ps the microcracks develop into a cluster of micropores that have lower potential energy due to the reduced area of internal free surfaces. With increasing energy deposited by the laser pulse, more substantial damage is produced. Microcracks crop out to the surface of the particle, Figure 3b, and, at energies deposited higher than ~0.14 eV per molecule, split the particle apart.<sup>14</sup>

In order to reveal the physical processes responsible for the laser damage to the particle we correlate the visual pictures shown in Figure 3 with the spatial and time development of the local hydrostatic pressure in the irradiated particles presented in Figure 4 in the form of contour plots. For the 15 ps laser pulse, a high compressive pressure (positive pressure in Figure 4) builds up in the central part of the particle during the laser pulse. This pressure is the result of inertial stress confinement, when the laser heating of the irradiated particle occurs faster than the mechanical relaxation of the thermoelastic stresses.<sup>1,5,7,8</sup> The minimum characteristic time of mechanical response to the heating can be estimated as the ratio of the size of the heating volume to the speed of acoustic wave propagation. For particles with a radius of ~55 nm and with a speed of sound in the 2D model of 2760 m/s, the time of mechanical relaxation is ~20 ps. Thus, the conditions for inertial confinement exist for 15 ps laser pulses and lead to the high pressure build up in the central part of the particle, Figure 4a. As a consequence of the laser induced compressive pressure an unloading wave propagates from the surface of the particle. Focusing of the unloading wave leads to the concentration of the tensile stresses in the center of the particle at ~50 ps, Figure 4a. The generation of the microcracks, Figure 3a, coincides temporally and spatially with the maximum tensile stresses, indicating that it is the tensile stresses that cause the damage of the particle.

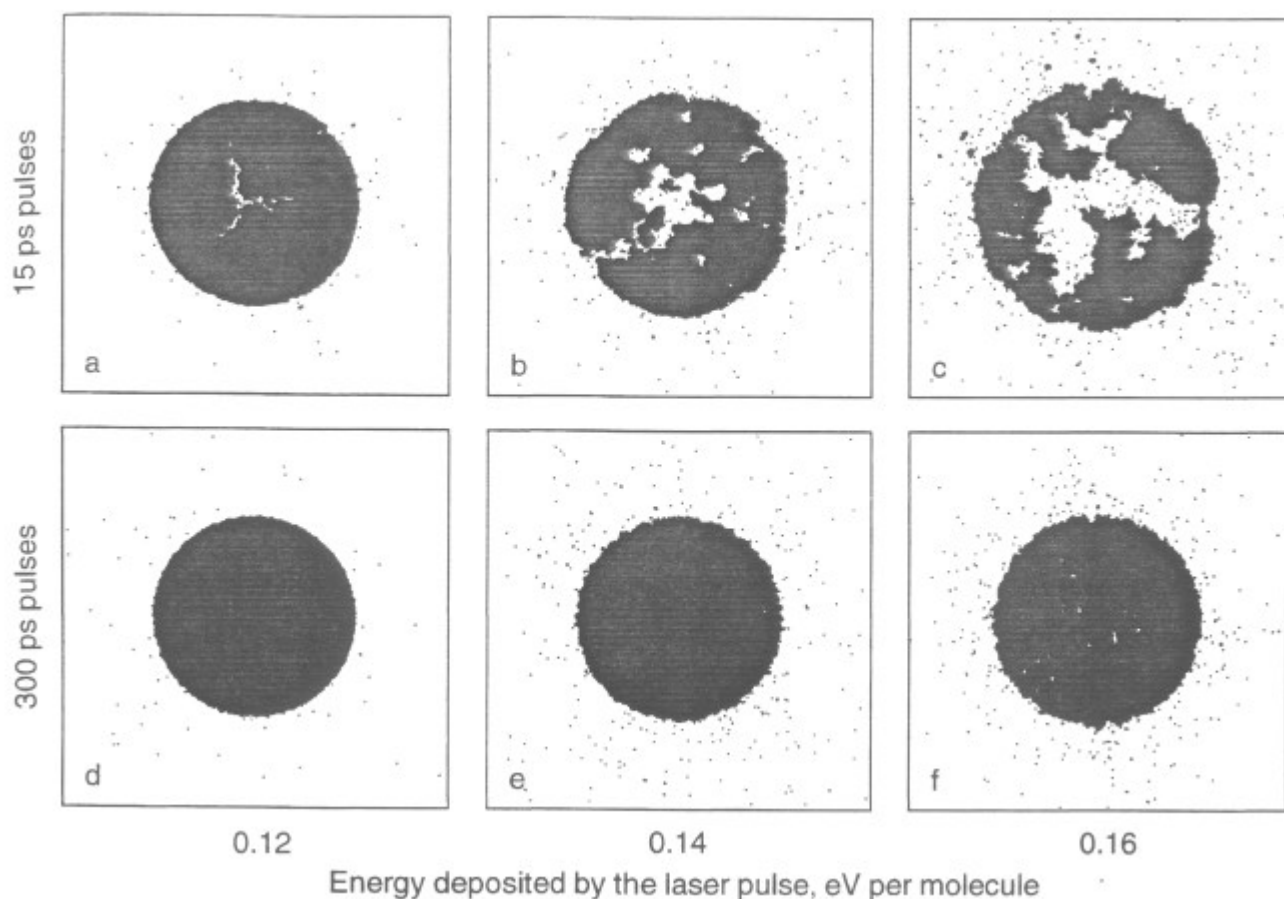


Figure 3. Snapshots from the MD simulations of isolated particles vs. deposited laser energy. Results at 200 ps after the end of the laser pulses are shown for 15 ps (a-c) and 300 ps (d-f) pulse durations.

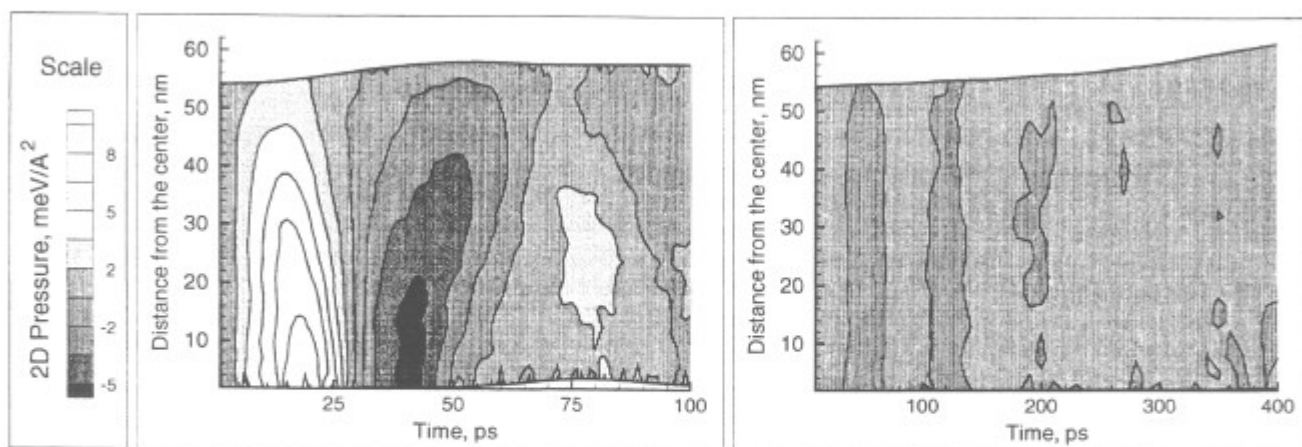


Figure 4. Spatial and time distribution of the local hydrostatic 2D pressure within the particles irradiated with (a) 15 ps and (b) 300 ps laser pulses. Energies deposited by the laser pulses are (a) 0.12 and (b) 0.16 eV per molecule. The contour plots are drawn through the points corresponding to the average of the local pressure for molecules in 20 ring-shaped zones within the particle. The data points are calculated at 1 ps intervals during the MD trajectories starting from the beginning of the laser pulse.

For the longer laser pulse, significantly higher laser fluences are required to cause a visible damage to the particle, Figure 3d-e. The pressure contour in Figure 4b shows that there is scarcely any pressure buildup induced by the 300 ps laser pulse even for the highest laser fluence shown in Figure 3. A 300 ps laser pulse is significantly longer than the time of mechanical relaxation of the particle and thermal expansion occurs during the energy deposition. Thus, the mechanical mechanism of particle damage and ablation that is crucial for 15 ps pulse irradiation does not play any role in the case of 300 ps pulses. For energy of 0.16 eV per molecule deposited, the onset of homogeneous melting and formation of small cavities at the end of the laser pulse is observed. An additional increase of the deposited energy leads to the overheating of the particle up to the limit of its thermodynamic stability,<sup>15</sup> when the particle spontaneously decomposes into a mixture of gas phase molecules and molecular clusters.<sup>14</sup>

This thermal decomposition or explosion leads to the transfer of a significant part of the deposited laser energy to the radial expansion of the disintegrated particle. This can be seen from the time dependence of the average kinetic energy of molecular motion in the radial and tangential directions shown for 3D simulations in Figure 5. The tangential component does not contain a contribution from the radial expansion of the overheated particle and can be associated with the thermal motion whereas the difference between radial and tangential parts of the kinetic energy corresponds to the energy of the radial flow apart. At high laser fluences, when an explosive disintegration of the overheated particles occurs, a splitting of the radial and tangential components of the kinetic energy is observed for both shorter and longer laser pulses as shown in Figure 5. Several points can be made regarding the figure. First, the phase explosion provides fast cooling of the particle and short time of the thermal spike. A big part of the thermal energy is transferred in this case into potential energy of particle decomposition and kinetic energy of the radial flow apart. Second, for the same laser energies deposited, the energy of radial expansion is significantly higher for the shorter laser pulses, when the inertially confined thermoelastic pressure adds to the pressure of the thermal explosion. Third, the transfer of the laser energy to the energy of radial expansion is much faster for the 10 ps pulse than for the 100 ps pulse. As shown in the next subsection, a stronger pressure wave with a steeper front is emitted into the surrounding medium as a result of the faster and stronger radial expansion of the absorbing particle for shorter pulses.

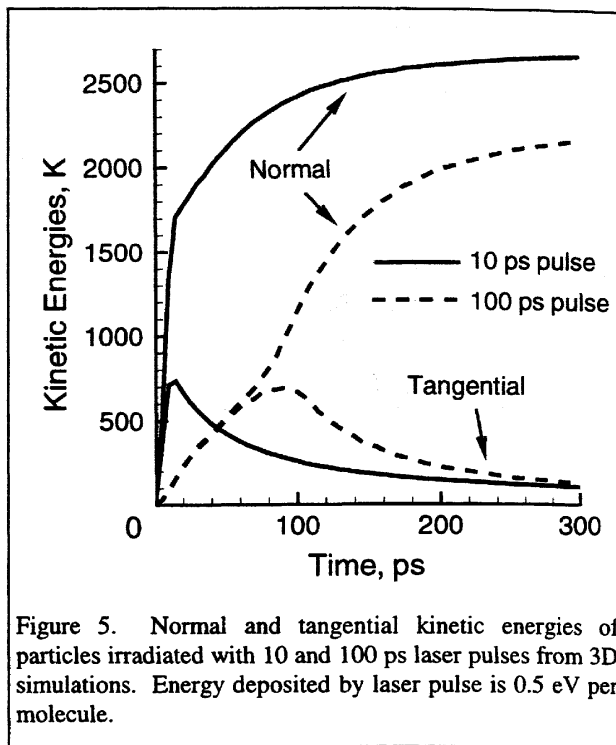


Figure 5. Normal and tangential kinetic energies of particles irradiated with 10 and 100 ps laser pulses from 3D simulations. Energy deposited by laser pulse is 0.5 eV per molecule.

### 3.2 Coupling of the acoustic and thermal pulses to the surrounding medium.

To study the coupling of the processes within the absorbing particles to the surrounding medium, 2D simulations are performed for different laser fluences, pulse durations and properties of the surrounding medium. The pressure and defect contour plots for three simulations with the same deposited energy of 0.2 eV per molecule are shown in Figure 6. The plots in Figure 6a are for the 300 ps laser pulse and the same intermolecular interaction within and outside the absorbing particle. A 300 ps laser pulse is longer than the time needed for thermal expansion to occur, and only a moderate pressure builds up in the hot particle by the end of the pulse. The slow thermal expansion does not cause any noticeable pressure wave in the surrounding medium and only a transitory appearance of a small number of defects is observed in the central part of the absorbing particle.

As discussed above for isolated particles, irradiation with the 15 ps laser pulse leads to a high compressive pressure build up during the pulse, Figure 6b. Relaxation of the compressive pressure leads to the emission of a strong pressure wave into the surrounding medium and propagation of an unloading wave from the border of the particle toward the center. The pressure wave in the medium carries a significant part of the absorbed laser energy away from the absorption site. This is illustrated in Figure 7 where the time development of the energy in the absorbing particle, within a 90 nm zone around the particle, and outside this zone is plotted. More than 30% of the absorbed laser energy is transferred from the absorbing particle to the surrounding medium during the first 100 ps after the laser pulse. Consequently less energy is left to induce mechanical or thermal damage within the particle. Although the energy deposited in this simulation is higher than for the

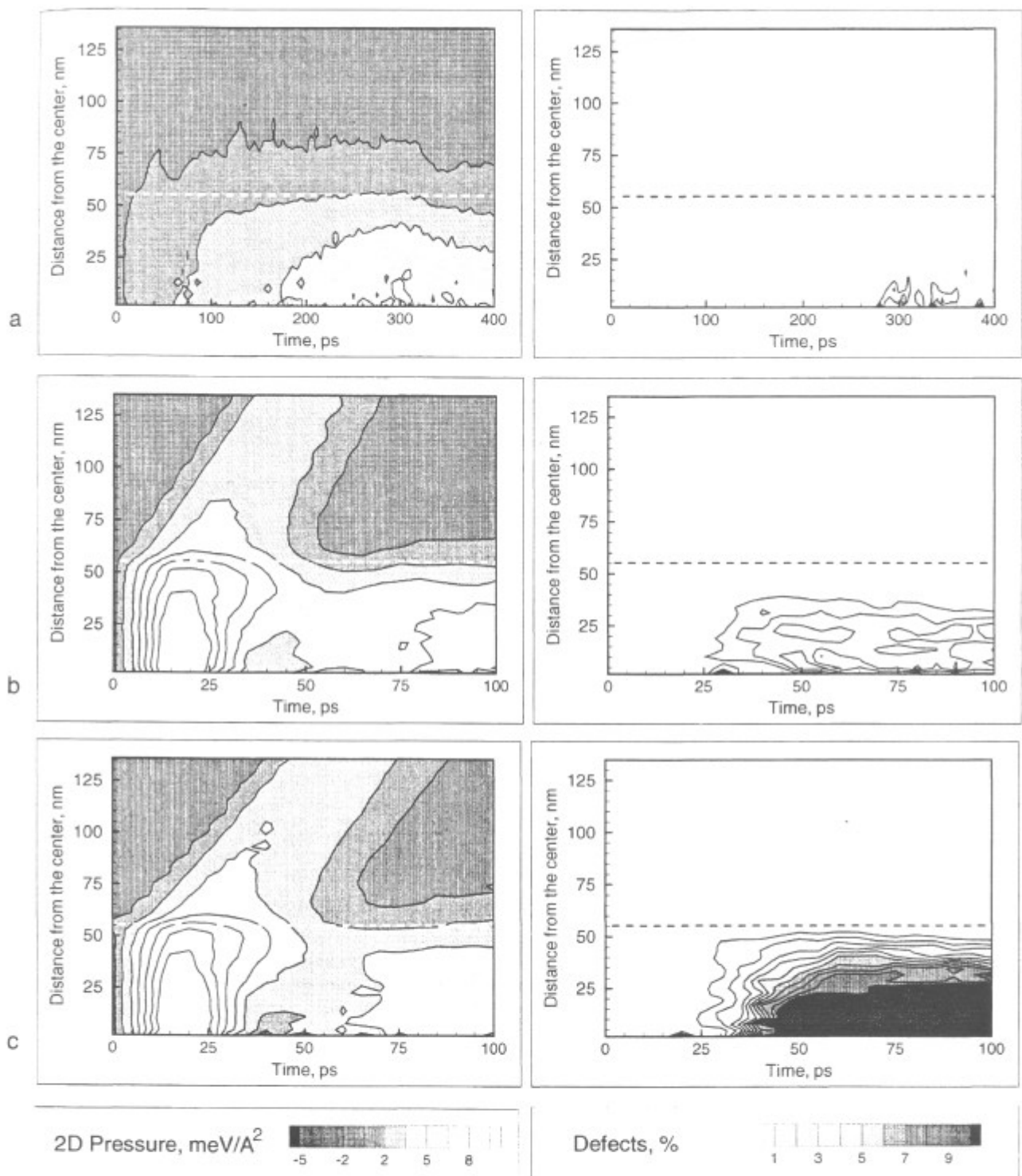


Figure 6. Spatial and time distribution of the local hydrostatic 2D pressure (left) and defect density (right) within and outside the absorbing particles embedded into a transparent medium. The contour plots are for the energy of 0.2 eV per molecule deposited by 300 ps (a) and 15 ps (b,c) laser pulses. Simulations are performed for the particles and surrounding medium with identical mechanical properties (a, b) and for the surrounding medium with intermolecular interactions twice as strong as within the absorbing particle (c). Dashed lines mark the boundary of the absorbing particle.

simulations shown in Figure 3, the defect density in Figure 6 is lower than the ones for isolated particles. Melting and formation of numerous small cavities rather than fracturing in the central part of the particle is responsible for the rise of the defect density in Figure 6b.

Simulations with two sets of parameters for intermolecular interactions in the surrounding medium are performed to investigate the role of the acoustic impedance mismatch at the interface between the absorbing granule and the surrounding medium. In the simulations when the granule and the surrounding medium have identical mechanical properties the most efficient transfer of the expansion energy into producing the pressure wave is observed, Figure 7. When the surrounding medium is weaker/softer than the absorbing particle, less energy goes out from the particle, Figure 7, and a higher defect density within the particle is observed, Figure 6c. Unloading wave that propagates from the border of the irradiated particle and focuses in the central region is stronger in the case of the softer surrounding medium and leads to the more significant pressure lowering. The reduced pressure facilitates cavitation within the overheated particle that is reflected in higher defect density in Figure 6c as compared to Figure 6b. The difference in mechanical properties of the absorbing particle and surrounding medium thus appears to define the role of the intragranular fracturing/cavitation in short pulse laser damage. The greater is the difference, the bigger part of the compressive pressure experience reflection at the interface and is transferred into the expansion wave that focuses in the center of the particle and cause cavitation or fracturing. The results for isolated particles with free boundary conditions, Figures 3 and 4, can be viewed as an extreme case of the maximum impedance mismatch at the particle/surround interface and the maximum photomechanical damage to the particles.

#### 4. Summary

The basic processes and mechanisms that define a low energy threshold for visible damage to pigmented tissues are studied using the MD method and the breathing sphere model. Different threshold energies and qualitative differences in the damage mechanisms for shorter, tens of picoseconds, and longer, hundreds of picoseconds, laser pulses are observed for both isolated particles and absorbing granules embedded in a transparent medium.

For the shorter pulses a high compressive pressure builds up in the irradiated particles under conditions of inertially confined photothermal expansion. Relaxation of the compressive pressure leads to the formation of a strong pressure wave that carries a significant part of the absorbed laser energy away from the absorption site. Upon interaction with intracellular structures the pressure wave has the potential to develop a tensile component and cause a photomechanical damage in the areas distant from the absorbing compounds. Within the absorbing granule, an unloading wave propagates from the boundary of the absorbing granule and focuses in the centre. The focusing leads to the expansion in the central part of the granule and causes fracturing or cavitation. This effect of intragranular mechanical damage becomes more pronounced with increasing acoustic impedance mismatch between granule and surrounding medium. Photomechanical damage due to the pressure wave emission from the absorbing granule and intragranular fracturing/cavitation can occur at the deposited energies significantly

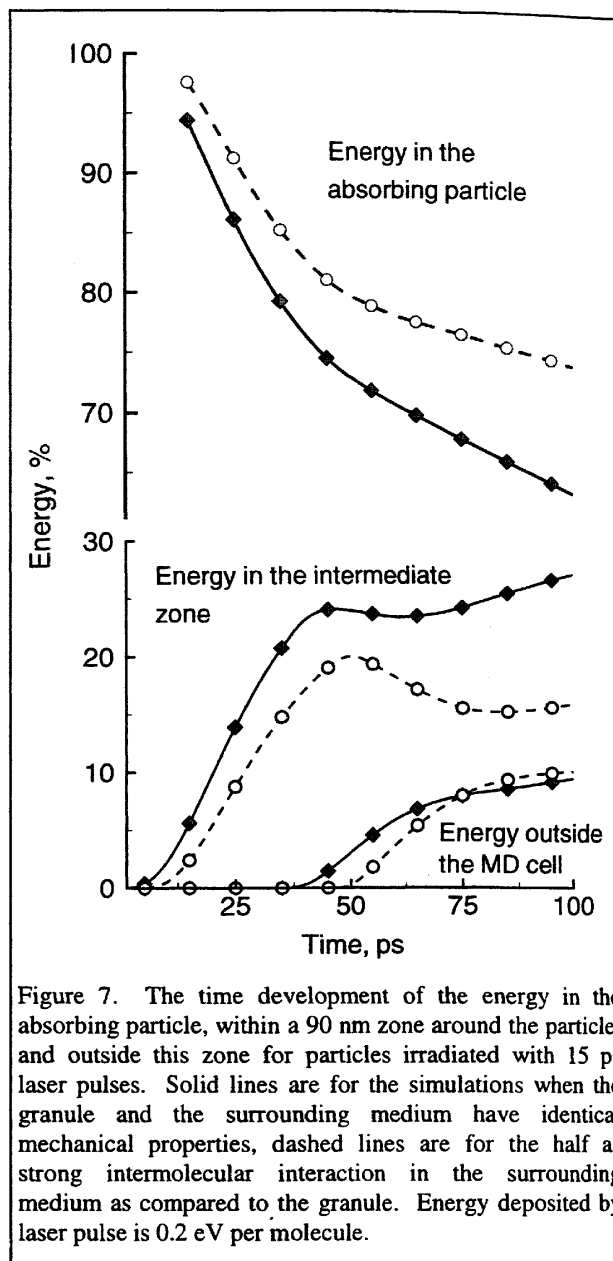


Figure 7. The time development of the energy in the absorbing particle, within a 90 nm zone around the particle, and outside this zone for particles irradiated with 15 ps laser pulses. Solid lines are for the simulations when the granule and the surrounding medium have identical mechanical properties, dashed lines are for the half as strong intermolecular interaction in the surrounding medium as compared to the granule. Energy deposited by laser pulse is 0.2 eV per molecule.



lower than the ones required for explosive vaporization of the absorption site and is likely to be responsible for the energetically efficient regime of the short pulse laser ablation of the tissue.

For the longer, hundreds of picoseconds, laser pulses thermal expansion occurs during the laser energy deposition and no high pressure build up and photomechanical effects are observed in the simulated energy range. Overheating of the absorbing granule up to the level for explosive vaporization is required to cause a visible damage.

The results from the simulation demonstrate the ability of the MD method and the breathing sphere model to provide insight into the basic microscopic mechanisms of short pulse laser damage at the absorption site and coupling of the processes within the absorbing granule to the surrounding medium. Experimental data on the molecular structure and properties of the intracellular components are needed for more detailed quantitative analysis of the threshold values and damage mechanisms. Combination of the present molecular level model with a continuum description can open the way for multiscale modeling of laser-tissue interactions.

### Acknowledgments

We gratefully acknowledge financial support from the Chemistry Division of the National Science Foundation. The computational support for this work was provided by the IBM-SUR Program and the Center for Academic Computing at Penn State University.

### References

1. S. L. Jacques, A. A. Oraevsky, R. Thompson, and B. S. Gerstman, "A working theory and experiments on photomechanical disruption of melanosomes to explain the threshold for minimal visible retinal lesions for sub-ns laser pulses," *Laser-Tissue Interaction V*, S. L. Jacques, Editor, Proc. SPIE **2134A**, pp. 54-65, 1994.
2. C. R. Thompson, B. S. Gerstman, S. L. Jacques, and M. E. Rogers, "Melanin granule model for laser induced thermal damage to the retina," *Bulletin Mathematical Biology* **58**, pp. 513-553, 1996.
3. C. P. Lin and M. W. Kelly, "Ultrafast time-resolved imaging of stress transient and cavitation from short pulsed laser irradiated melanin particles," *Laser-Tissue Interaction VI*, S. L. Jacques, Editor, Proc. SPIE **2391**, pp. 294-299, 1995.
4. M. W. Kelly and C. P. Lin, "Microcavitation and cell injury in RPE cells following short-pulsed laser irradiation," *Laser-Tissue Interaction VIII*, S. L. Jacques, Editor, Proc. SPIE **2975**, pp. 174-179, 1997.
5. M. Strauss, P. A. Amendt, R. A. London, D. J. Maitland, M. E. Glinsky, C. P. Lin, and M. W. Kelly, "Computational modeling of stress transient and bubble evolution in short-pulse laser irradiated melanosome particles," *Laser-Tissue Interaction VIII*, S. L. Jacques, Editor, Proc. SPIE **2975**, pp. 261-270, 1997.
6. D. W. Heermann, *Computer Simulation Methods in Theoretical Physics*, Berlin: Springer-Verlag, 1990.
7. L. V. Zhigilei, P. B. S. Kodali, and B. J. Garrison, "Molecular dynamics model for laser ablation of organic solids," *J. Phys. Chem. B* **101**, pp. 2028-2037, 1997.
8. L. V. Zhigilei, P. B. S. Kodali, and B. J. Garrison, "On the threshold behavior in the laser ablation of organic solids," *Chem. Phys. Lett.* **276**, pp. 269-273, 1997.
9. L. V. Zhigilei and B. J. Garrison, "Velocity distributions of molecules ejected in laser ablation," *Appl. Phys. Lett.* **71**, pp. 551-553, 1997.
10. M. E. Glinsky, D. S. Bailay, and R. A. London, "LATIS modeling of laser induced midplane and backplane spallation," *Laser-Tissue Interaction VIII*, S. L. Jacques, Editor, Proc. SPIE **2975**, pp. 374-387, 1997.
11. R. S. Dingus, D. R. Curran, A. A. Oraevsky, and S. L. Jacques, "Microscopic spallation process and its potential role in laser-tissue ablation," *Laser-Tissue Interaction V*, S. L. Jacques, Editor, Proc. SPIE **2134A**, pp. 434-445, 1994.
12. L. V. Zhigilei and B. J. Garrison, "Simple non-reflecting boundary conditions for elastic waves in molecular dynamics simulations," in preparation.
13. S.-P. Chen, T. Egami, and V. Vitek, "Local fluctuations and ordering in liquid and amorphous metals," *Phys. Rev. B* **37**, pp. 2440-2449, 1988.
14. L. V. Zhigilei and B. J. Garrison, "Computer simulation study of damage and ablation of submicron particles from short pulse laser irradiation," *Applied Surface Science* **125**, March issue, pp. xxxx, 1998.
15. R. Kelly and A. Miotello, "Comments on explosive mechanisms of laser sputtering," *Applied Surface Science* **96-98**, pp. 205-215, 1996.